Journal of Medicinal Chemistry Article

J. Med. Chem. **2010,** *53,* 7337–7343 **7337**
DOI: 10.1021/jm100585j

Light Induced Antimicrobial Properties of a Brominated Boron Difluoride (BF_2) Chelated Tetraarylazadipyrromethene Photosensitizer

Daniel O. Frimannsson, Marco Grossi, Julie Murtagh, Francesca Paradisi, and Donal F. O'Shea*

Centre for Synthesis and Chemical Biology, School of Chemistry and Chemical Biology, University College Dublin, Belfield, Dublin 4, Ireland

Received May 13, 2010

Herein we describe a new antimicrobial photodynamic therapeutic (PDT) agent based upon the brominated BF_2 chelated tetraarylazadipyrromethene photosensitizer class. Bis-ammonium salt substitution of the photosensitizer promoted a rapid 10 min uptake into Gram-positive and -negative bacterial strains and pathogenic yeasts. A photosensitizer and light dose response analysis for methicillin-sensitive *S. aureus* showed an impressive antibacterial efficacy with 1, 2, and 5 μg/mL **6**. Specifically, light activation with a dose of 16 J/cm^2 and 5 μg/mL **6** resulted in a 6.8 and 3.4 $\log_{10}$ reduction of *S. aureus* and a clinically defined methicillin-resistant *Staphylococcus aureus* (MRSA) strain, respectively. Encouragingly, a broad spectrum pathogen response (using 5 μg/mL **6** and 75 J/cm^2) was observed with 3.6 and 5.7 $\log_{10}$ decreases in viable cell numbers achievable for Gram-negative bacterium *E. coli* and the pathogenic yeast *C. albicans*, respectively. The photophysical and cell eradicating characteristics of this bis-cationic PDT agent suggest that it has broad potential in antimicrobial therapeutics.

Introduction

The continuing emergence of an increasing number of resistant bacterial strains toward penicillins and streptomycin has sparked an exhaustive effort in developing alternative treatment strategies. Some examples involve modifying the structures of existing antimicrobial agents, while new motifs are being pursued through natural product screening.[1] However, the threat of potential resistance against these new agents is a constant concern.[2] For that reason, alternative efforts have been focused on finding different strategies that would show activity against a broad spectrum of pathogens, including resistant bacterial and fungal strains. One such strategy that has received attention for the treatment of localized infection is photodynamic therapy (PDT[a]).

PDT is a treatment that uses a combination of two relatively nontoxic components, visible light and a photosensitizer, to exert an antiproliferating effect. The process involves activating the photosensitizer by irradiation with low energy light at a wavelength range of 650−700 nm. The excited photosensitizer can react with molecular oxygen to locally produce toxic reactive oxygen species (ROS) or directly with surrounding biomolecules, ultimately providing the cytotoxic effects via oxidative damage.[3] This unique mode of disease treatment using a combination of light, photosensitizer, and oxygen has expanded from an initial clinical focus for oncological diseases to include conditions such as age-related macular degeneration and microbial infections.[4] Specifically for microbial infection, inherent selectivity advantages can be gained by this approach, as the excitation light can be delivered accurately to the area under treatment and the photosensitizer can be structurally designed to have some inherent selectivity for microbial cell uptake. Neutral and anionic photosensitizer are generally taken up by and inactivate Gram-positive species, whereas the addition of membrane disorganizing agents such as ethylenediaminetetraacetic acid or the nonapeptide polymyxin B is needed to photoinactivate Gram-negative species.[5,6] Recent examples have shown that the photosensitization of both Gram-negative and positive bacteria is achievable with cationic photosensitizer without the addition of membrane disorganizing agents.[7] Consequently, the focus has shifted toward the development of positively charged photosensitizers that could be utilized for clinical applications such as wound disinfection, periodontal disease, and blood sterilization.[8] Despite the numerous PDT agents that have been tested in vivo for activity against cancer, there have been relatively few reports of their use to treat bacterial infections in vivo. Hamblin et al.[9] utilized the poly-L-lysine-chlorin$_{e6}$ conjugate **1a** to illustrate the photoinactivation of *Escherichia coli* in wounds, where the treatment did not damage the host tissue (Figure 1). Additionally, **1a** showed activity against *Pseudomonas aeruginosa* infected wounds in vivo and restrained the bacteria from entering the bloodstream, indicating the possibility of a treatment of wound and other localized infections.[10] A related polyethyleneimine analogue **1b** has also shown comparable antimicrobial photoinactivation and supplementary resistance to enzymatic hydrolysis of the lysine−lysine peptide bonds of **1a**.[11] PDT with **1b** was shown to elicit a 2.7 $\log_{10}$ of inactivation of methicillin-resistant *Staphylococcus aureus* (MRSA) in skin abrasion wounds using a mouse model.[12]

Recently, conjugation of the cationic antimicrobial peptide apidaecin to a *meso*-tetraarylporphyrin provided a new agent class with potent broad spectrum activity.[13] The bis-ammonium

*To whom correspondence should be addressed. Phone: +353-1-7162425. E-mail: donal.f.oshea@ucd.ie.

[a] Abbreviations: PDT, photodynamic therapy; MRSA, methicillin-resistant *Staphylococcus aureus*; DPBF, 1,3-diphenylisobenzofuran; SDS, sodium dodecyl sulfate; ROS, reactive oxygen species; $OD_{650\ nm}$, optical density at 650 nm; log *P*, partition coefficient between distilled water and 1-octanol.

Published on Web 09/29/2010

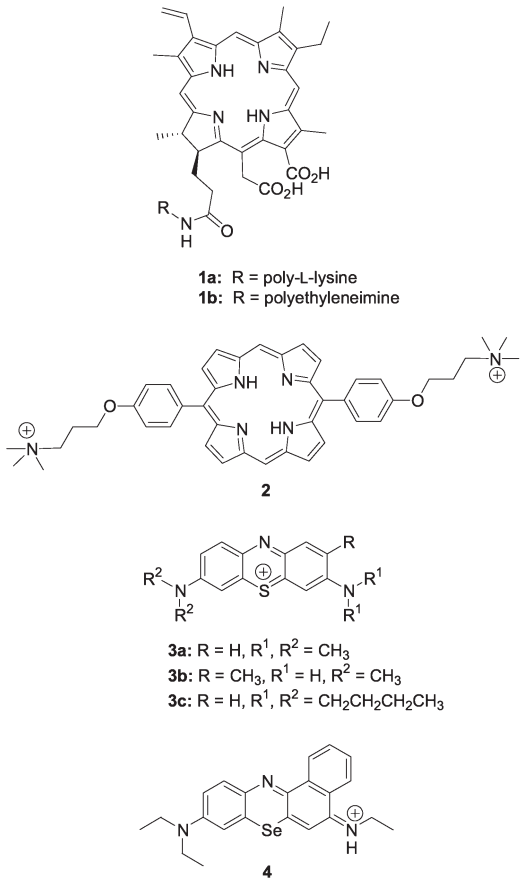

Figure 1. Antibacterial PDT agents.

salt *meso*-substituted porphyrin **2** has been shown to exhibit a high degree of potency against Gram-positive bacteria at concentrations that have minimal effect on eukaryotic cells.[14] Phenthiazinium derivatives such as methylene blue **3a** and toluidine blue **3b** have been successfully tested for photoinactivation of blood pathogens, and the former has been used to decontaminate fresh frozen blood plasma.[15,16] Recently, **3a** has also been successfully used to eradicate MRSA strains in superficial and deep wounds in mice models.[17] The treatment lead to a 14-fold reduction in the number of viable bacteria without affecting the surrounding host tissue. Teichert et al. have also used **3a** to treat *Candida albicans* infections in immunodeficient mice, mimicking Cronic candidiasis, a condition commonly found in patients infected by human immunodeficiency virus.[18] Toluidine blue **3b** has also received considerable attention as a PDT agent, especially against oral infections.[19,20] Furthermore, treatment with **3b** was shown to be highly effective in vivo against *Vibrio vulnificus*, an extremely virulent bacterium.[21] The authors concluded that the photoactivity acted partly by reducing the bacterial virulence factors in the wound. A further related derivative of methylene blue **3c** is currently in phase II clinical trial for the treatment of chronic leg ulcers.[22] A series of three chalcogen substituted benzo[*a*]phenoxazinium analogues have been reported that have increasing phototoxicity depending on substitution.[23] The progression of the phototoxicity is attributable to the heavy atom effect, as the selenium-substituted chalcogen **4** showed the most efficient phototoxicity against both *Enterococcus faecalis* and *E. coli*. It was also shown that compound **4** was taken up by the parasitic strain *Leishmania major* and caused its death upon irradiation, further demonstrating

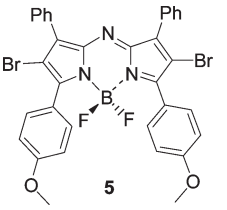

Figure 2. Antitumor brominated BF_2-chelated tetraarylazadipyrromethene.

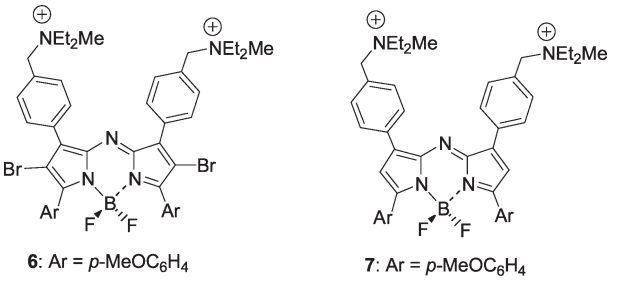

Figure 3. Antimicrobial brominated BF_2-chelated tetraarylazadipyrromethene **6** and its nonbrominated analogue **7**.

the possibility of using PDT against a diverse variety of pathogens.[24]

We have previously reported the development of a novel class of non-porphyrin based PDT agents, termed the brominated BF_2-chelated tetraarylazadipyrromethenes. We have shown in vitro that compound **5** has excellent photophysical characteristics and EC_{50} values in the low nanomolar range with numerous tumor cell types (Figure 2).[25] Moreover, these novel photosensitizers show very low dark toxicity.[26] Studies using a MDA-MB-231 human breast cancer tumor model in mice showed tumor ablation in 71% of animals after iv delivery of **5** (2 mg/kg) followed immediately by irradiation with a 150 J/cm^2 light fluence.[27] Critically, the synthesis of this photosensitizer class is relatively straightforward and results in defined single agents. They are amenable to modification around the periphery of the sensitizer, thus allowing for optimization of all aspects of their photophysical and therapeutic properties. Herein, we describe the tailoring of this sensitizer class for specific application to eradication of a broad spectrum of microbial cells.

Results and Discussion

Photosensitizer Design. To customize the BF_2-chelated tetraarylazadipyrromethene class for antimicrobial PDT, we envisaged a design that involved the substitution of the sensitizer with cationic quaternary ammonium salt functional groups. As such, the bis-cationic structure **6** was selected for synthesis and its ability to elicit a light induced antimicrobial effect determined (Figure 3). It was anticipated that the bis-ammonium salt would impart sufficient water solubility for routine use without the requirement of additional solubilizing agents and the amphiphilic nature of the sensitizer would promote microbial cellular uptake.

Parallel to **6**, the structurally related nonbrominated analogue **7** was used for examination of the cellular uptake and for fluorescence imaging because of its expected superior fluorescence quantum yield. We have previously shown that the inclusion of bromine atoms at the β-pyrrole positions of this sensitizer class leads to elevated ROS generation and a

Scheme 1. Synthetic Route to **6**

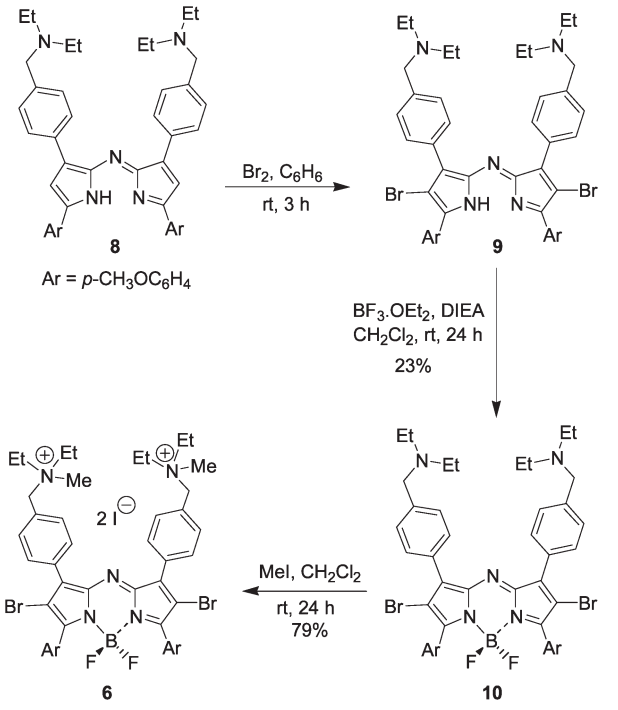

lower fluorescence quantum yield with respect to the nonbrominated analogues.[25]

Synthesis. The starting point for the synthesis of **6** was the previously reported bis-amine substituted azadipyrromethene **8** which is readily available in three routine steps from 4-diethylaminomethyl benzaldehyde and 4-methoxyacetophenone (Scheme 1).[28] The room temperature bromination of **8** with bromine efficiently produced the bis-brominated derivative **9** which was directly transformed into its corresponding BF_2-chelated **10** by reaction with boron trifluoride and diisopropylethylamine in CH_2Cl_2. The final step involved the alkylation of the bis-amine with iodomethane in CH_2Cl_2 at room temperature, producing the desired product **6** in high yield. Recrystallization from dichloromethane/diethyl ether gave the final product as a dark green solid. A closely related synthetic route to produce **7** (omitting the bromination step) has been previously reported.[29]

Photophysics. The absorption spectra of **6** and **7** in methanol show wavelengths of maximum absorbance at 681 and 702 nm, respectively, which are in an ideal spectral range for use as antibacterial PDT agents (Table 1). The emission λ_{max} values of **6** and **7** were recorded at 722 and 732 nm, respectively, with the dibrominated **6** having a considerably lower fluorescence quantum yield of 0.1 when compared to 0.22 for **7** (Table 1). This reflects the general behavior of this class which shows a lower fluorescence quantum yield as a result of the bromination at the β-pyrrole positions. This heavy-atom effect indicates the potential use of **6** as a PDT agent and **7** as a near-infrared fluorescence imaging probe.[25]

A photo-oxidation study using **6** and **7** was undertaken by monitoring the light induced degradation of 1,3-diphenylisobenzofuran (DPBF) with sensitizer generated ROS. This was achieved experimentally by irradiating solutions containing photosensitizer (1×10^{-8} M) and DPBF (initial concentration of 5×10^{-5} M) and following the disappearance of the absorbance band of the latter at 415 nm over a time period of 45 min. A fiber optic delivered filtered light of

Table 1. Spectroscopic and Physical Properties of **6** and **7**

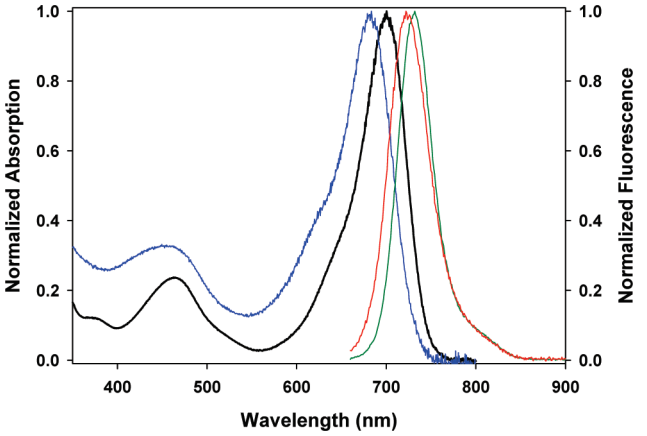

sensitizer	λ_{max} abs (nm)[a,b]	ε (M^{-1} cm^{-1})[c]	λ_{max} flu (nm)[a,d]	Φ_f[c]	log P[e]
6	681 (blue)	64 000	722 (red)	0.10	−0.25
7	702 (black)	69 000	732 (green)	0.22	−0.45

[a] In MeOH. [b] 1×10^{-5} M. [c] In $CHCl_3$. [d] 5×10^{-6} M. [e] Partition coefficient between distilled water and 1-octanol.

wavelength 620 ± 30 nm was used to mimic those utilized for our in vitro assays or for future clinical therapy. Methylene blue **3a** (1×10^{-8} M) was chosen as a comparative reference from which relative rates of ROS production could be determined because of its related use in antibacterial PDT.[25] Encouragingly, as shown in panel A of Figure 4, photosensitizer **6** proved to be a highly efficient producer of ROS with a DPBF degradation profile comparable to that of methylene blue (panel B). The relative rates of DPBF degradation under these conditions were determined and were found to be in a ratio of 1.1:1 for **3a**/**6** (Supporting Information Figure S1). In stark contrast, the nonbrominated **7** failed to produce any significant amount of ROS above that generated in the absence of a photosensitizer (Figure 4, panels C and D).

This photophysical phenomenon is again attributable to the heavy-atom effect induced by the bromine atoms in **6**. This subtle structural difference permits the use of the higher fluorescence quantum yield of **7** for fluorescence imaging and uptake studies and the use of **6** for cell killing assays. An examination of the photostability and oxidation stability of photosensitizer **6** showed it to be remarkably stable under irradiation conditions. Irradiation of 1.6×10^{-5} M aerated solution of **6** as described above in the absence of the DPBF quencher caused only a slow degradation of the sensitizer as judged by UV−visible analysis with 91%, 78%, and 65% of the sensitizer remaining after 15, 30, and 45 min respectively (Supporting Information Figure S2).

Uptake Studies. On the basis of ROS generation and fluorescence quantum yield, fluorophore **7** was utilized to determine uptake by various different cell types using fluorescence spectroscopy and confocal microscopy. As such, various microbial cells were incubated with **7** at a concentration of 5 μg/mL (4.9 μM) for 10 min at room temperature. The cells were then washed twice with phosphate buffered saline (PBS pH 7.4) to remove unbound **7** and lysed with 10% sodium dodecyl sulfate (SDS) to extract the bound fluorophore. The percentage of fluorophore taken up was determined by fluorescence intensity of the extracted

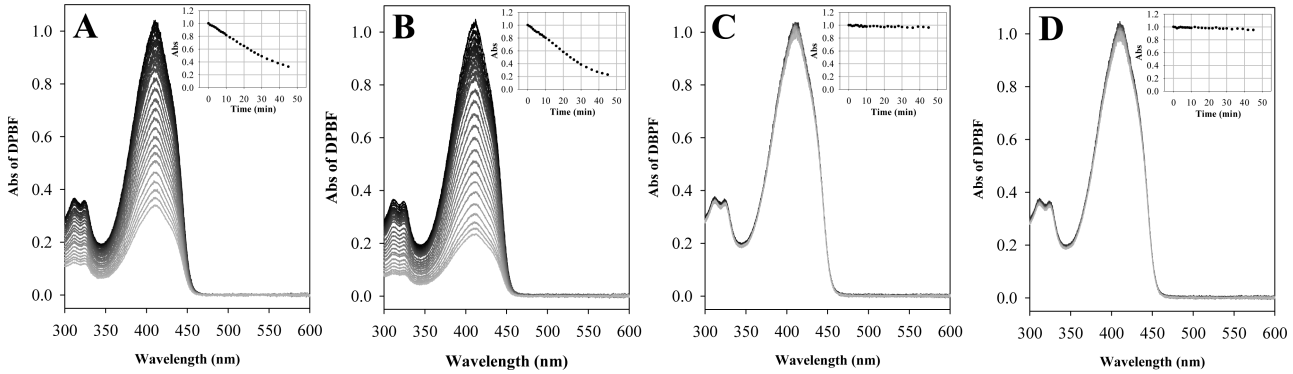

Figure 4. Comparative DPBF degradation profiles by **6** (A), **3a** (B), **7** (C), and no photosensitizer (D). Concentration of **3a**, **6**, and **7** at 1×10^{-8} M and DPBF initially at 5×10^{-5} M in acetonitrile.

Table 2. Uptake of **7** in Prokaryotic and Eukaryotic Cells[a,b]

	strain				
	S. aureus[c]	MRSA	*E. coli*	*C. albicans*	MDA-MB-231
bound fraction	49%	31%	80%	25%	0.3%

[a] 5 μg/mL (4.9 μM). [b] Incubation at room temperature for 10 min. [c] Methicillin-sensitive strain.

solution compared to a calibration plot of known concentrations in 10% SDS solution. The Gram-positive bacteria *S. aureus* showed almost 50% uptake after 10 min of incubation, while the MRSA strain showed relatively less at 31% (Table 2). Furthermore, very efficient uptake by the Gram-negative bacteria *E. coli* was observed after 10 min of incubation, while the larger *C. albicans* yeast cells showed 25% uptake. Most encouragingly from a selectivity point of view, when the uptake by these pathogens is compared to that of the human MDA-MB-231 cell line, the human cells showed a minimal uptake after 10 min of incubation, indicating preferential uptake by bacterial cells within this short time frame (Table 2).

In addition, the microbial uptake was examined by confocal laser scanning microscopy. The obtained images shown in Figure 5 confirm that **7** was indeed internalized over the broad spectrum of microbes after only 10 min of incubation, and this could be readily monitored with a fluorescence microscope systems. While no distinct subcellular localization patterns could be discerned for **7** in Gram-positive strains, it was notable that in *E. coli* the staining pattern was throughout the cell but appeared more intense at the outer peripheral edge indicative of the cell wall (Figure 5, panels a−c, Supporting Information Figures S3 and S4). Images of *C. albicans* showed a more granular cellular distribution (panel d).

The partition coefficients between distilled water and 1-octanol (log *P*) of **6** and **7** were measured as −0.25 and −0.45, respectively, which are comparable to that of methylene blue **3a** (Table 1).[30] The efficient uptake of our compound class could be attributed to a combination of the biscationic amphiphilic nature of the compounds coupled with log *P* values close to zero.

Light Induced Toxicity Studies. The initial evaluation of the photodynamic potential of **6** was determined by using a methicillin-sensitive *S. aureus* strain. Cells were incubated in the dark at room temperature for 10 min (based on the uptake studies of **7**) with sensitizer concentrations of 1, 2, and 5 μg/mL (corresponding to 0.85, 1.7, and 4.3 μM respectively). The cells were washed to remove unbound

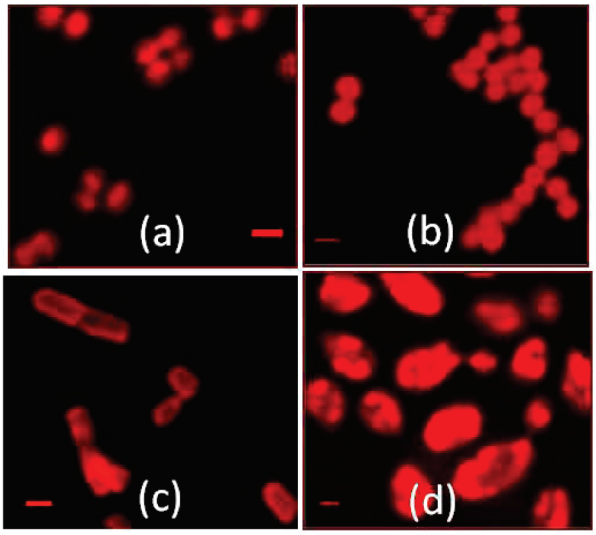

Figure 5. Confocal laser scanning microscopy images of (a) *S. aureus*, (b) MRSA, (c) *E. coli*, (d) *C. albicans* after 10 min of incubation with **7** (5 μg/mL, 4.9 μM). Excitation wavelength was 633 nm, and fluorescence was detected using a long-pass filter at 650 nm. Scale bars are 1 μm.

sensitizer and irradiated with varying light doses from 0 to 16 J/cm^2 using a filtered light source with wavelength of 690 ± 25 nm. This treatment regime resulted in both light and concentration dependent cell killing as expected for a PDT response (Figure 6, Table 3). For example, at the 1 μg/mL dosage of **6** in the absence of light (0 J/cm^2) no cell death was observed. Following light dose irradiations of 2, 4, 8, and 16 J/cm^2 $\log_{10}$ reductions in viable *S. aureus* cell numbers of 0.1, 0.3, 1.4, and 3.0, respectively, were obtained (Table 3; Figure 6, black dotted line). Utilizing a sensitizer **6** and light dose of 2 μg/mL and 16 J/cm^2 gave an improved $\log_{10}$ cell reduction of 3.9 (Figure 6, black dashed line). Increasing the concentration of **6** to 5 μg/mL led to a 6.8 $\log_{10}$ eradication (> 99.9999% cell killing) after the delivery of 15 J/cm^2 light (Figure 6, black solid line). In each case experiments could be compared to a control that received light alone (Figure 6, gray line). In correlation with the comparative ROS study discussed in the previous section, the nonbrominated **7** was shown to be totally ineffective at inducing cell death even after 25 J/cm^2 light treatment (Supporting Information Figure S5).

As a long-term advantage of antimicrobial PDT lies in its broad-spectrum activity, we next examined the phototoxicity

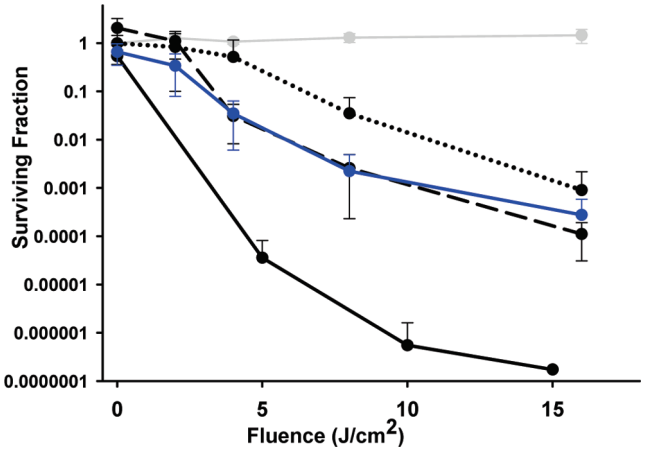

Figure 6. Light induced toxicity of **6** against *S. aureus* (10^8 units/mL): control 0 μg/mL (gray trace), 1 μg/mL (dotted black trace), 2 μg/mL (dashed black trace), 5 μg/mL (solid black trace) and against MRSA (10^8 units/mL) 5 μg/mL (solid blue trace). Data are expressed as the mean ± SEM from three independent experiments performed in triplicate.

Table 3. Broad-Spectrum Efficacy of **6**[a]

organism	**6** dose (μg/mL)	light dose (J/cm^2)	$\log_{10}$ reduction[b]
S. aureus[c]	1[d]	0	0
S. aureus[c]	1[d]	2	0.1
S. aureus[c]	1[d]	4	0.3
S. aureus[c]	1[d]	8	1.4
S. aureus[c]	1[d]	16	3.0
S. aureus[c]	2[e]	16	3.9
S. aureus[c]	5[f]	15	6.8
MRSA	5[f]	16	3.4
E. coli	5[f]	75	3.6
C. albicans	5[f]	75	5.7

[a] Incubation at room temperature for 10 min. [b] The $\log_{10}$ reductions of the viable cell numbers were determined by the CFU assay. Control experiments without illumination have shown that these concentrations have no antimicrobial activity under the same conditions. [c] Methicillin-sensitive strain. [d] 0.85 μM. [e] 1.7 μM. [f] 4.3 μM.

of **6** against a variety of different microbes, including pathogenic strains at a 5 μg/mL level with varying light dose. A clinical isolated methicillin-resistant *S. aureus* (MRSA) strain showed a >99.9% (3.4 $\log_{10}$) cell killing after 16 J/cm^2 light treatment, which is relatively less than the methicillin-sensitive *S. aureus* strain (Figure 6, blue trace, Table 3). This difference in efficacy is consistent with the measured sensitizer uptake in the two different strains as shown in the previous section which could potentially be attributable to subtle cell-wall differences.[31]

The light-dose response results obtained for the Gram-negative *E. coli* and yeast *C. albicans* strains with 5 μg/mL **6** are illustrated in Figure 7. Previous reports with other structural classes of photosensitizer have illustrated that both Gram-negative and yeast strains are generally less susceptible to PDT than Gram-positive strains.[8] Yet we were encouraged to observe that *E. coli* showed nearly a 99.99% cell eradication following the administration of a 75 J/cm^2 light dose (Figure 7, black trace, Table 3). The requirement of higher light dose to achieve a 3.6 $\log_{10}$ eradication cannot be attributed to an ineffective uptake of the photosensitizer but perhaps to its less uniform distribution within the cell. Lastly, *C. albicans* yeast cells were used to determine the effect of photodynamic treatment of **6** (5 μg/mL, 4.3 μM) on larger eukaryotic cells. Following light irradiation (75 J/cm^2)

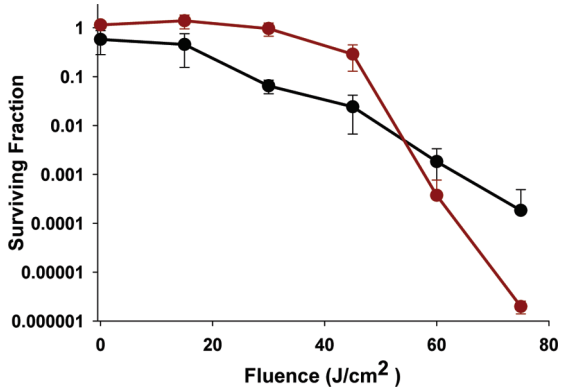

Figure 7. Light induced toxicity of **6** at 5 μg/mL (4.3 μM) against *E. coli* (10^8 units/mL) (black trace) and the pathogenic yeast *C. albicans* (10^8 units/mL) (brown trace). Data are expressed as the mean ± SEM of values from three independent experiments performed in triplicate.

a very effective PDT response was observed with close to a 99.9999% (5.7 $\log_{10}$) of *C. albicans* cell death (Figure 7, brown trace, Table 3). The requirement of an initial light dose, of 40 J/cm^2 in our case, prior to the induction of cell death is a feature previously observed for PDT killing of *C. albicans*.[32]

Conclusion

A new bis-cationic BF_2-chelated tetraarylazadipyrromethene **6** has been developed that shows significant potential as a new antimicrobial photodynamic therapeutic agent capable of eradicating a broad spectrum of pathogens. The absorption spectrum of **6** is optimal for application as an antimicrobial PDT agent, and its efficient production of ROS is attributable to the inclusion of bromine substituents on the pyrrole rings. By use of the related nonbrominated fluorescent analogue **7**, it was possible to illustrate a rapid uptake of this compound class into Gram-positive and Gram-negative strains of bacteria and a known pathogenic fungal strain. Encouragingly, only minimal binding was observed to a human cell line after the short incubation period. Photosensitizer **6** was shown to be highly phototoxic to various strains of pathogens, even the Gram-negative strain that is generally believed to be more resistant to the effects of photodynamic antibacterial therapy. In conclusion, this new agent may serve as an important addition to the emerging field of photodynamic antimicrobial therapy and the results described herein are encouraging for the further in vivo testing of these compounds against localized infections.

Experimental Section

General Information and Materials. The bacterial strains used in this study were *E. coli* BL21 (DE3), *S. aureus* ATCC 6538, and *C. albicans* SC5314, and the clinical isolate of MRSA was collected by, and the antibiotic susceptibility determined at, the clinical microbiology laboratory of Beaumont Hospital, Dublin, Ireland. Synthetic reaction conditions and yields are not optimized. Chromatography was performed using Apollo 60/40 silica gel and Merck alumina 90. Chemical shifts are reported in parts per million (ppm) and referenced to $CDCl_3$. Infrared spectra were recorded as a KBr thin film. Mass spectrometry was acquired using a micromass time-of-flight spectrometer. On the basis of NMR and reverse phase HPLC, all final compounds are >95% pure.

BF_2 Chelate of *N*-(4-(4-Bromo-2-(4-bromo-3-(4-((diethyl(methyl)-ammonio)methyl)phenyl)-5-(4-methoxyphenyl)-1*H*-pyrrol-2-ylimino)-5-(4-methoxyphenyl)-2*H*-pyrrol-3-yl)benzyl)-*N*-ethyl-*N*-methylethanaminium Iodide (6). Compound **10** (100 mg, 0.11 mmol) was dissolved in dry CH_2Cl_2 (20 mL), treated with methyl iodide (175 μL, 2.8 mmol), and stirred under N_2 for 24 h at room temperature. Diethyl ether (20 mL) was added, and the formed precipitate was filtered, washed with diethyl ether, and dried. The product was obtained as a dark green solid (101 mg, 79%), mp > 300 °C. ^{1}H NMR (500 MHz, $CDCl_3$) δ: 7.77−7.75 (m, 4H), 7.70−7.67 (m, 8H), 6.90 (d, J = 9.0 Hz, 4H), 5.37 (s, 4H), 3.86 (s, 6H), 3.72−3.65 (m, 4H), 3.47−3.40 (m, 4H), 3.17 (s, 6H), 1.55 (t, J = 7.0 Hz, 12H). ^{13}C NMR (125 MHz, $CDCl_3$) δ: 161.9, 157.7, 143.9, 140.9, 133.0, 132.7, 132.5, 130.9, 129.7, 128.1, 121.2, 113.6, 110.6, 63.4, 55.5, 55.3, 47.2, 8.9. IR (KBr disk): 3433, 1641 cm^{-1}. ES-MS: m/z 1040.5 $[M - I^-]^+$, $C_{46}H_{52}BBr_2F_2IN_5O_2^+$. HRMS $[M - I^-]^+$: 1040.1633, $C_{46}H_{52}BBr_2F_2IN_5O_2^+$ requires 1040.1594.

Fluorescence Quantum Yield Measurements. Fluorescent quantum yields for **6** and **7** were determined in chloroform using BF_2 chelate of [5-(4-methoxyphenyl)-3-phenyl-1*H*-pyrrol-2-yl]-[5-(4-methoxyphenyl)-3-phenylpyrrol-2-ylidene]amine as a reference with Φ_f of 0.36.[25]

Comparative DPBF Degradation Measurements. A 100 mL constantly aerated acetonitrile solution containing **3a**, **6**, or **7** at a concentration of 1×10^{-8} M and 1,3-diphenylisobenzofuran at an initial concentration of 5×10^{-5} M was irradiated with a 150 W fiber optic delivered filtered light (620 ± 30 nm) at 25 °C for 45 min. Aliquots of 2 mL were removed from the solution every 1 min for the first 10 min, every 2 min for the following 20 min, and every 3 min for the last 15 min, and a UV−visible spectrum was recorded. Degradation of 1,3-diphenylisobenzofuran was monitored by the decrease in absorbance intensity at 415 nm.

Photobleaching Measurement. A 100 mL constantly aerated acetonitrile solution of **6** at 1.6×10^{-5} M was irradiated with a 150 W fiber optic delivered filtered light (620 ± 30 nm) at 25 °C for 45 min. Aliquots of 2 mL were removed from the solution every 5 min for 45 min, and a UV−visible spectrum was recorded. Degradation of **6** was judged by a decrease in absorption λ_{max} at 680 nm.

Cell Culture. Luria−Bertani (LB) medium was used for *S. aureus* and *E. coli*. A single colony was used to inoculate 10 mL of liquid medium. Cells were grown at 37 °C under aerobic conditions on a shaker incubator (200 rpm) until an OD_{600nm} of approximately 0.7 was reached. YM medium was used for *C. albicans*, and the fungal cells were grown to an approximate OD_{600nm} of 0.6 (10-fold dilution was measured). MDA-MB-231 cells were cultured at 37 °C in the presence of 5% CO_2 in Dulbecco's modified Eagle's medium (DMEM) supplemented with 10% fetal calf serum, 20 U/mL penicillin, and 50 μg/mL streptomycin.

Photosensitizer Solution. Solutions for uptake and photodynamic inactivation studies were freshly prepared by dissolving the desired compound in a 25% methanol in phosphate buffered saline solution (PBS 1×, pH 7.4) to make a stock solution of 100 μg/mL.

Uptake Studies. For bacteria and yeast, an aliquot (1000 μL) of liquid medium containing grown cells was collected into an Eppendorf and centrifuged (8500*g*, 1 min). The cells were then resuspended in PBS (950 μL) to give the appropriate cell density (OD_{600nm} of 0.7 for *S. aureus*, MRSA, and *E. coli* and OD_{650nm} of 0.6 for the 10-fold dilution of *C. albicans*). Compound **7** (100 μg/mL) was added (50 μL) to give a final concentration of 5 μg/mL (4.9 μM), and the suspension was incubated at room temperature in the dark for 10 min. After the incubation period, this suspension was centrifuged (8500*g*, 1 min) and resuspended in PBS (1000 μL). The suspension was centrifuged again (8500*g*, 1 min), and the remaining pellets were lysed in 10% SDS aqueous solution (1000 μL). This solution was incubated at room temperature overnight before absorbance and fluorescence were measured. The measurements were collected from three independent experiments performed in triplicate. Similarly, the MDA-MB-231 human carcinoma cell line was seeded in a 12-well plate at a concentration of approximately 5×10^6 cells/mL in serum containing DMEM and allowed to attach for 24 h. A fresh solution of **7** diluted in DMEM cell culture media was added (1000 μL) to give a final concentration of 5 μg/mL (4.9 μM). The cells were then incubated for 10 min at room temperature and then washed twice with PBS before being suspended in 10% SDS and analyzed as described above.

Photodynamic Inactivation Studies. An aliquot of cells culture (1000 μL) at the appropriate cell density (OD_{600nm} of 0.7 for *S. aureus*, MRSA, and *E. coli* and OD_{650nm} of 0.6 for *C. albicans*) was collected and centrifuged (8500*g*, 1 min). The cell pellets were resuspended in PBS (990, 980, or 950 μL). The photosensitizer under study (100 μg/mL in PBS, pH 7.4) was added (10, 20, or 50 μL) to give the desired concentration (1, 2, or 5 μg/mL), and the suspension was incubated at room temperature in the dark for 10 min. The cells were then centrifuged (8500*g*, 1 min) and resuspended in PBS (1000 μL) twice to remove the unbound photosensitizer. Aliquots of this suspension (200 μL) were placed into a 96-well plate. Before irradiation, an aliquot (20 μL) was taken from a well to determine the colony forming units in the absence of light. During irradiation, aliquots (20 μL) were removed from the wells at specific time points corresponding to specific fluences. In order to determine the colony forming units, each aliquot was diluted with liquid medium to 10^{-1}−10^{-6} times the original concentration, and each dilution was streaked horizontally on a square LB medium (or yeast rich medium for *C. albicans*) agar plate as described by Jett et al.[33] The plates were then incubated at 37 °C overnight, the colonies were counted, and the survival fraction was determined from the untreated control in the absence of light. A LumaCare LC-122 M fiber optic noncoherent light delivery system emitting light at 690 nm (±25 nm) was used to deliver light with an irradiance measured to be 20 mW/cm^2 for the lower fluency rates and 120 mW/cm^2 for the higher ones. Experiments were carried out in triplicate and at three independent occasions.

Confocal Laser-Scanning Microscopy. Cells were suspended in PBS to give the appropriate cell density (OD_{600nm} of 0.7 for *S. aureus*, MRSA, and *E. coli* and OD_{650nm} of 0.6 for the 10-fold dilution of *C. albicans*), then treated with compound **7** at a final concentration of 5 μg/mL (4.9 μM) for 10 min at room temperature. The cells were then washed twice with PBS by centrifugation (8500*g*, 1 min), and a drop of the suspension was placed onto a glass slide and allowed to dry before a coverslip was mounted on the slide. Fluorescent images were then collected with a confocal laser scanning microscopy (LSM510, Carl Zeiss) using an excitation wavelength of 633 nm and a band-pass filter at 650 nm.

Acknowledgment. This work was supported by grants from Science Foundation Ireland and The Irish Research Council for Science, Engineering and Technology. Thanks are extended to H. Humphreys and J. O'Gara for MRSA, G. Butler for *C. albicans*, W. Gallagher for MDA-MB-231 cells.

Supporting Information Available: Synthesis procedure and analytical data for compound **10**; NMR spectrum and HPLC trace of **6**; DPBF degradation rate plots; confocal microscopy Z-stack images of *E. coli* and *S. aureus*; photobleaching of **6**; and PDT assay data plot for **7** on *S. aureus*. This material is available free of charge via the Internet at http://pubs.acs.org.

References

(1) Coates, A.; Hu, Y.; Bax, R.; Page, C. The future challenges facing the development of new antimicrobial drugs. *Nat. Rev. Drug Discovery* **2002**, *1*, 895–910.

(2) Mulvey, M. R.; Simor, A. E. Antimicrobial resistance in hospitals: how concerned should we be? *Can. Med. Assoc. J.* **2009**, *180*, 408–415.
(3) Wainwright, M. Photodynamic antimicrobial chemotherapy (PACT). *J. Antimicrob. Chemother.* **1998**, *42*, 13–28.
(4) Maisch, T. Antimicrobial photodynamic therapy: useful in the future? *Lasers Med. Sci.* **2007**, *22*, 83–91.
(5) Bertolini, G.; Rossi, F.; Valduga, G.; Jori, G.; Lier, J. Photosensitizing activity of water- and lipid-soluble phthalocyanines on *Escherichia coli*. *FEMS Microbiol. Lett.* **1990**, *71*, 149–155.
(6) Nitzan, Y.; Gutterman, M.; Malik, Z.; Ehrenberg, B. Inactivation of Gram-negative bacteria by photosensitized porphyrins. *Photochem. Photobiol.* **1992**, *55*, 89–96.
(7) Merchat, M.; Bertolini, G.; Giacomini, P.; Villanueva, A.; Jori, G. Meso-substituted cationic porphyrins as efficient photosensitizers of Gram-positive and Gram-negative bacteria. *J. Photochem. Photobiol., B* **1996**, *32*, 153–157.
(8) Maisch, T. A new strategy to destroy antibiotic resistant microorganisms: antimicrobial photodynamic therapy. *Mini-Rev. Med. Chem.* **2009**, *9*, 974–983.
(9) Hamblin, M. R.; O'Donnell, D. A.; Murthy, N.; Contag, C. H.; Hasan, T. Rapid control of wound infections by targeted photodynamic therapy monitored by in vivo bioluminescence imaging. *Photochem. Photobiol.* **2002**, *75*, 51–57.
(10) Hamblin, M. R.; Zahra, T.; Contag, C. H.; McManus, A. T.; Hasan, T. Optical monitoring and treatment of potentially lethal wound infections in vivo. *J. Infect. Dis.* **2003**, *187*, 1717–1725.
(11) Tegos, G. P.; Anbe, M.; Yang, C.; Demidova, T. N.; Satti, M.; Mroz, P.; Janjua, S.; Gad, F.; Hamblin, M. R. Protease-stable polycationic photosensitizer conjugates between polyethyleneimine and chlorin(e6) for broad-spectrum antimicrobial photoinactivation. *Antimicrob. Agents Chemother.* **2006**, *50*, 1402–1410.
(12) Dai, T.; Tegos, G. P.; Zhiyentayev, T.; Mylonakis, E.; Hamblin, M. R. Photodynamic therapy for methicillin-resistant *Staphylococcus aureus* infection in a mouse skin abrasion model. *Lasers Surg. Med.* **2010**, *42*, 38–44.
(13) Dosselli, R.; Gobbo, M.; Bolognini, E.; Campestrini, S.; Reddi, E. Porphyrin−apidaecin conjugate as a new broad spectrum antibacterial agent. *ACS Med. Chem. Lett.* **2010**, *1*, 35–38.
(14) Maisch, T.; Bosl, C.; Szeimies, R.-M.; Lehn, N.; Abels, C. Photodynamic effects of novel XF porphyrin derivatives on prokaryotic and eukaryotic cells. *Antimicrob. Agents Chemother.* **2005**, *49*, 1542–1552.
(15) Mohr, H.; Lambrecht, B.; Selz, A. Photodynamic virus inactivation of blood components. *Immunol. Invest.* **1995**, *24*, 73–85.
(16) Wainwright, M.; Mohr, H.; Walker, W. H. Phenothiazinium derivatives for pathogen inactivation in blood products. *J. Photochem. Photobiol., B* **2007**, *86*, 45–58.
(17) Zolfaghari, P. S.; Packer, S.; Singer, M.; Nair, S. P.; Bennett, J.; Street, C.; Wilson, M. In vivo killing of *Staphylococcus aureus* using a light-activated antimicrobial agent. *BMC Microbiol.* **2009**, *9*, 27.
(18) Teichert, M. C.; Jones, J. W.; Usacheva, M. N.; Biel, M. A. Treatment of oral candidiasis with methylene blue-mediated photodynamic therapy in an immunodeficient murine model. *Oral Surg., Oral Med., Oral Pathol. Oral Radiol., Endodontol.* **2002**, *93*, 155–160.
(19) Wilson, M. Lethal photosensitisation of oral bacteria and its potential application in the photodynamic therapy of oral infections. *Photochem. Photobiol. Sci.* **2004**, *3*, 412–418.
(20) Wilson, M.; Dobson, J.; Harvey, W. Sensitization of oral bacteria to killing by low-power laser radiation. *Curr. Microbiol.* **1992**, *25*, 77–81.
(21) Wong, T. W.; Wang, Y. Y.; Sheu, H. M.; Chuang, Y. C. Bactericidal effects of toluidine blue-mediated photodynamic action on *Vibrio vulnificus*. *Antimicrob. Agents Chemother.* **2005**, *49*, 895–902.
(22) http://clinicaltrials.gov/ct2/show/study/NCT00825760.
(23) Foley, J. W.; Song, X.; Demidova, T. N.; Jalil, F.; Hamblin, M. R. Synthesis and properties of benzo[*a*]phenoxazinium chalcogen analogues as novel broad-spectrum antimicrobial photosensitizers. *J. Med. Chem.* **2006**, *49*, 5291–5299.
(24) Akilov, O. E.; Kosaka, S.; O'Riordan, K.; Song, X.; Sherwood, M.; Flotte, T. J.; Foley, J. W.; Hasan, T. The role of photosensitizer molecular charge and structure on the efficacy of photodynamic therapy against Leishmania parasites. *Chem. Biol.* **2006**, *13*, 839–847.
(25) Gorman, A.; Killoran, J.; O'Shea, C.; Kenna, T.; Gallagher, W. M.; O'Shea, D. F. In vitro demonstration of the heavy-atom effect for photodynamic therapy. *J. Am. Chem. Soc.* **2004**, *126*, 10619–10631.
(26) Gallagher, W. M.; Allen, L. T.; O'Shea, C.; Kenna, T.; Hall, M.; Gorman, A.; Killoran, J.; O'Shea, D. F. A potent nonporphyrin class of photodynamic therapeutic agent: cellular localisation, cytotoxic potential and influence of hypoxia. *Br. J. Cancer* **2005**, *92*, 1702–1710.
(27) Byrne, A. T.; O' Connor, A.; Hall, M.; Murtagh, J.; O' Neill, K.; Curran, K. M.; Mongrain, K.; Rousseau, J. A.; Lecomte, R.; McGee, S.; Callanan, J. J.; O'Shea, D. F.; Gallagher, W. M. Vascular targeted photodynamic therapy with BF_2-chelated tetraaryl-azadipyrromethene agents. *Br. J. Cancer* **2009**, *101*, 1565–1573.
(28) McDonnell, S. O.; Hall, M. J.; Allen, L. T.; Byrne, A.; Gallagher, W. M.; O'Shea, D. F. Supramolecular photonic therapeutic agents. *J. Am. Chem. Soc.* **2005**, *127*, 16360–16361.
(29) Tasior, M.; Murtagh, J.; Frimannsson, D. O.; McDonnell, S. O.; O'Shea, D. F. Water-solubilised BF_2-chelated tetraarylazadipyrromethenes. *Org. Biomol. Chem.* **2010**, *8*, 522–525.
(30) Wainright, M. Methylene blue derivatives—suitable photoantimicrobials for blood product disinfection. *Int. J. Antimicrob. Agents* **2000**, *16*, 381–394.
(31) Kawai, M.; Yamada, S.; Ishidoshiro, A.; Oyamada, Y.; Ito, H.; Yamagisgi, J. Cell-wall thickness: possible mechanism of acriflavine resistance in meticillin-resistant *Staphylococcus aureus*. *J. Med. Microbiol.* **2009**, *58*, 331–336.
(32) Zeina, B.; Greenman, J.; Purcell, W. M.; Das, B. Killing of cutaneous microbial species by photodynamic therapy. *Br. J. Dermatol.* **2001**, *144*, 274–278.
(33) Jett, B. D.; Hatter, K. L.; Huycke, M. M.; Gilmore, M. S. Simplified agar plate method for quantifying viable bacteria. *BioTechniques* **1997**, *23*, 648–650.